Proceedings

Geohazards

Engineering Conferences International *Year* 2006

The Importance of Laboratory Experiments in Landslide Investigation

Barbara Schneider-Muntau*　　D. Renk†

T. Marcher‡　　Wolfgang Fellin**

*AlpS -GmbH, Center for Natural Hazard Management, schneider@alps-gmbh.com

†AlpS -GmbH, Center for Natural Hazard Management

‡ILF – Consulting Engineers

**Institute of Geotechnical and Tunnel Engineering, University Innsbruck, wolfgang.fellin@uibk.ac.at

The Importance of Laboratory Experiments in Landslide Investigation

B. Schneider-Muntau[1,2,3], D. Renk[1,3], T. Marcher[2], W. Fellin[3]

[1] AlpS - GmbH, Center for Natural Hazard Management, Grabenweg 3, A - 6020 Innsbruck; Email: schneider@alps-gmbh.com
[2] ILF – Consulting Engineers, Feldkreuzstr. 3, A - 6063 Rum, Austria
[3] Institute of Geotechnical and Tunnel Engineering, University Innsbruck, Technikerstr. 13, A - 6020 Innsbruck; Email: wolfgang.fellin@uibk.ac.at

Abstract

This study focuses on a better understanding of mass movements and on the influences of different boundary conditions on velocities of creeping slopes. A well monitored example of a slowly creeping landslide is the mass movement *Hochmais - Atemkopf*, situated in the Kaunertal, Tyrol, Austria (Fig. 1). The long term monitoring program for more than 40 years of this landslide gives a good impression of its time dependent behaviour. A large amount of additional data, as geological mapping, boreholes, geophysical investigation and so on provides a funded base for the model's geometry. The most influencing factor for finite element calculations is besides the model's geometry the rheological model and the therefor adapted material properties. Creep laboratory experiments have been performed and evaluated for the most active sliding zone. Long term shear tests from 1964 have been reevaluated and compared with current long term triaxial tests. The experiments reveal a non linear dependence between equivalent stress and displacement rate. An elasto, visco - plastic rheological model with a non linear viscose deformation has been fitted to those results.

Introduction

The slope under consideration is a more than 1000 m high mass movement in paragneiss rock in the Tyrolean Alps (Fig. 1). More than 40 years of geodetical measurement and extensometer data is available, which documents the slope's movement. The displacement vectors are mostly aligned parallel and indicate the major movements in the lower part of the slope (Fig. 2). With field mapping, geophysical investigations and borehole data the geological model was set up (Brückl et al., 2004). Four different sliding masses separated by assumed sliding zones could be determined (Fig. 1 and 2). Postglacially, a paragneiss slab came to lie on till, which now forms the sliding zone of the lowest and most active part of the slope. The volume of this slap is about 11 x 10^6 m^3 (Tentschert, 1998). The

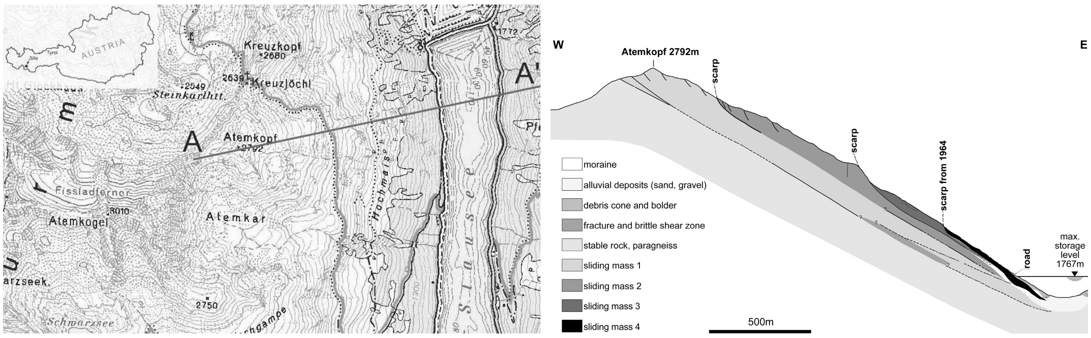

Figure 1: Geographic exposure and geological section A - A'

Table 1: Material properties

Material	Density	*Young's* Modulus	*Poisson's* ration	Friction-angle	Cohesion
	[kN/m^2]	[MN/m^2]	[-]	[°]	[MN/m^2]
Till	24	5	0.33	32	0
Paragneiss	28	39	0.25	45	20

other sliding zones consist in densely fractured and crushed paragneiss. To be able to build an appropriated numerical model, not only the geometry of the mass movement has to be known, also the material properties have to be determined. Material properties of the rock matrix are compiled from literature (Müller, 1963, 1992; Semprich and Plischke, 1984; Spickermann et al., 2003), the properties of the fractured rock mass have been calculated with the approach for rock classification according to Hoek (1999) for weathered rock, the strength parameters for the till originate from laboratory tests (Breth, 1967; Renk, 2006), see Tab. 1, and the nonlinear viscose material properties have been fitted to several creep tests.

Geodetical measurements

General overview

The whole slope is equipped with geodetic monitoring points (Fig. 2). Some of them are measured several times a day as basis of a monitoring system. In the lower part of the slope an investigation adit has been built which intersects the sliding zone and where an extensometer records the relative displacements of the lowest shell. The deformation measurements (Fig. 2) suggest that the slope is mainly in a secondary creep stage. The secondary creep stage is characterized by a linear creep deformation over time at constant stresses.

Seasonal dependencies of slope movement

The linear creep trend is superimposed by some cyclic movement (Fig. 2). Those cyclic movements are due to seasonally fluctuating influences, as storage water level and ground water flow and show a yearly acceleration in spring and a de-

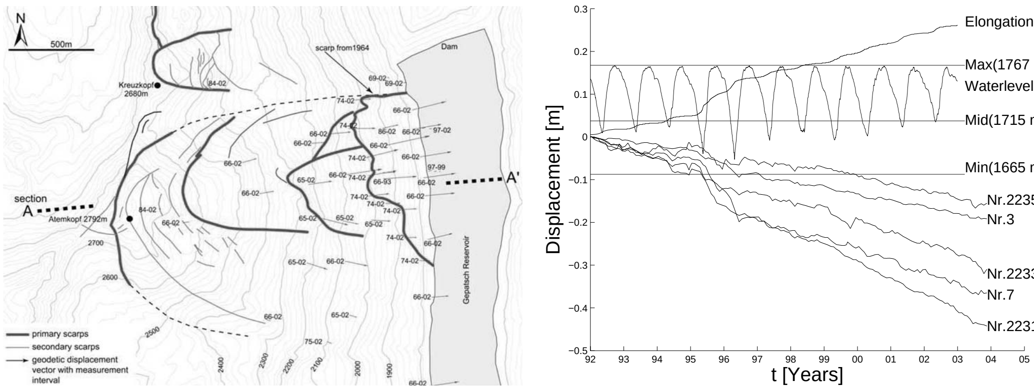

Figure 2: Geodetic points and measurements

Table 2: Displacement rates of the slope

	Total displacement	Displacement rate in spring (3 months) v_2	Displacement rate in the rest of the year (9 months) v_1
Year with high displacement	3.8 cm/year	10.8 cm/year	1.5 cm/year
Year with lower displacement	1.8 cm/year	3.6 cm/year	1.2 cm/year

celeration in autumn. Evaluating the slope movement for two exemplary years (1996 and 1998), two different slope velocities for each year can be approximated. With the end of January, begin of February, the slope accelerates. After three to four months of faster movement the slope decelerates and returns to its base activity. Those two motions are now regarded separately. In years with higher displacement rates (3.8 cm/year) 70% of the displacement takes place in the three spring months, in years with smaller displacement rates (1.8 cm/year) only 50% of the displacement (Tab. 2). The ratios of slope movement in spring to slope movement during the rest of the year v_2/v_1 are in between 3.0 - 7.2.

Laboratory experiment

Different bore holes were drilled and material of the sliding zone of the lowest part has been gained. Various laboratory experiments have been carried out on this material (TU Darmstadt, 1964; Renk, 2006). The long term creep tests are of particular interest in this case.

Creep test in shear box
The shear tests have been performed in 1964 at the technical University of Darmstadt. The shear test apparatus is made of two not connected frames (Fig. 3, top). A gap of few millimeters is left between those two frames in which the deformation

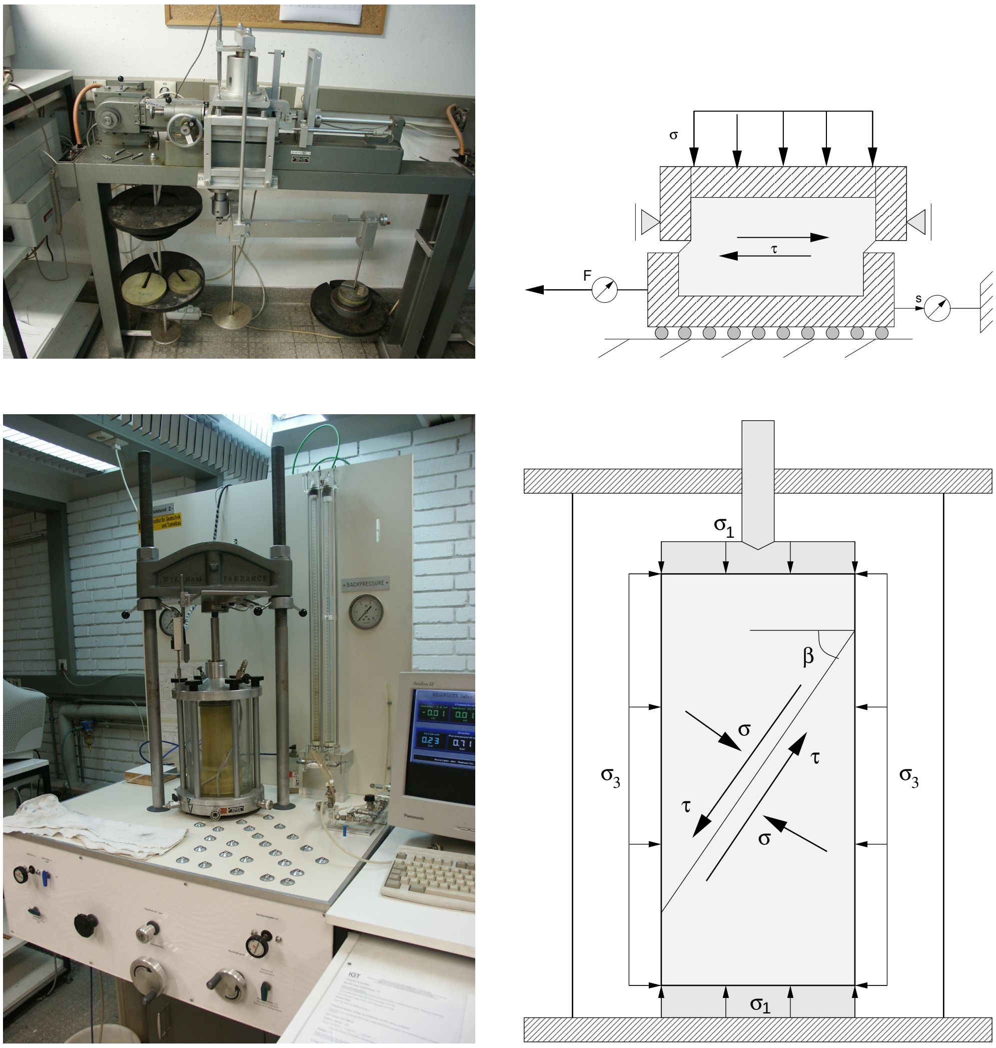

Figure 3: Shear test (top) and triaxial test (bottom)

takes place. The sample is loaded vertically and subsequently the lower frame is pulled horizontally. It is assumed that the shear stress is acting in the gap and the sample deforms because of the shear strains in the gap. The loads and the displacement of the moving frame are measured at regular time intervals. Three shear tests have been consolidated and vertically loaded with 500 kN/m^2 and the fourth with 300 kN/m^2. The shearing was carried out at constant shear stresses (55 kN/m^2, 110,kN/m^2, 155 kN/m^2 and 78 kN/m^2).

Triaxial creep tests
To investigate a three dimensional stress state the triaxial apparatus is more convenient. The sample is loaded horizontally and vertically. A shear band can develop without constrains within the sample (Fig. 3, bottom right). The load, the vertical displacement and the volume deformation are measured at regular

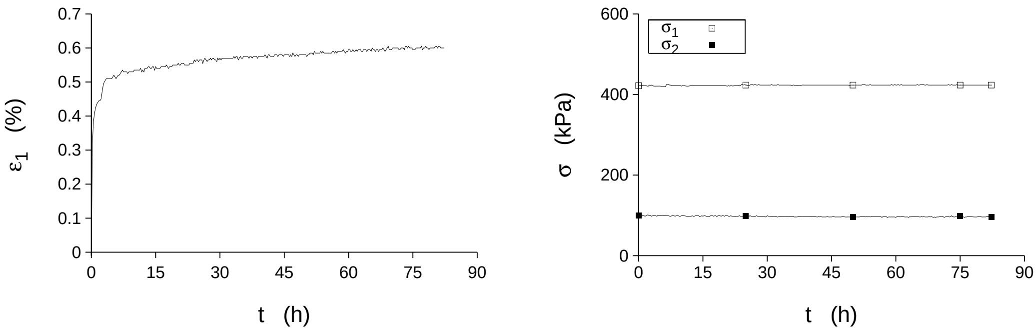

Figure 4: Strain - time curve with linear range and stress - time curve

time intervals. The triaxial test have been performed with a horizontal loading of 100 kN/m^2 and a vertical loading of 60%, 70%, 80% and 90% of the vertical strength.

Rheological model

A viscose rheological model has to be used in the numerical model to be able to reproduce time dependent deformation. The chosen rheological model was the *Bingham* model with and additional spring for elastic deformation. The equivalent stress has to be higher than the yield stress to allow viscose deformation. Below the yield stress only elastic deformation occurs. The *Bingham* model follows following equation:

$$\dot{\overline{\varepsilon}} = \frac{1}{\eta}(\overline{q} - q_y)^n \tag{1}$$

with the equivalent creep strain rate $\dot{\overline{\varepsilon}} = \sqrt{\frac{2}{3}\dot{\varepsilon} : \dot{\varepsilon}}$, the strain rate tensor $\dot{\varepsilon}$, the *Mises* equivalent stress $\overline{q} = \sqrt{\frac{3}{2}\mathbf{S} : \mathbf{S}}$, the deviatoric stress tensor $\mathbf{S}$, the yield stress q_y, the viscosity η (material property) and the exponent n (material property).

An exponent $n > 1$ causes an over linear dependence of the displacement rates on the stresses.

Laboratory results

The laboratory experiments have been evaluated in the linear range of the strain - time curve (Fig. 4).

Evaluation of the shear tests
As has been mentioned earlier, it is assumed that the shear strain is due to shear stresses in the gap between the two frames and is therefor a one dimensional problem. Applying the chosen rheological model, the shear tests can be evaluated

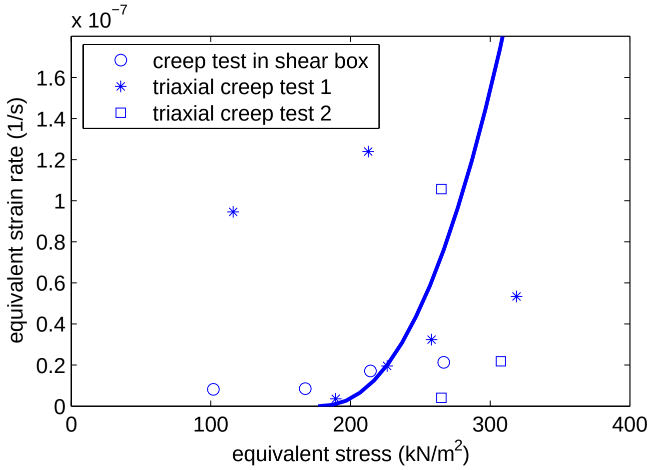

Figure 5: Correlation of creep strain rate with deviatoric stress

according to equation 1 as follows:

$$\overline{q} = \tau, \dot{\overline{\varepsilon}} = \dot{\gamma}, \gamma = \frac{s}{d}$$

with the shear strain rate $\dot{\gamma}$, the shear stress τ, the shear displacement s and the gap $d = 1.5$ mm in this case.

Evaluation of the triaxial tests
The triaxial tests are evaluated as three dimensional main stress state according to equation 1 as a three dimensional problem.

$$\overline{q} = \sigma_1 - \sigma_2, \dot{\overline{\varepsilon}} = \frac{2}{3}(\dot{\varepsilon_1} - \dot{\varepsilon_2})$$

Summary of the laboratory experiments
In total, 13 creep test have been performed so far. A potential function can be fitted to those results (Fig. 5). The equation that represents this regression is:

$$\dot{\overline{\varepsilon}} = 2 \cdot 10^{-12}(\overline{q} - 177)^{2.2}$$

Finite Element calculations

Model
The finite element calculation was performed using ABAQUS[1], version 6.5. Triangle elements with a second-order (quadratic) interpolation are used to get good results in spite of the small ratio of the narrow sliding zone to the slope's length (Schneider-Muntau et al., 2006).

[1]©2005 Abaqus, Inc

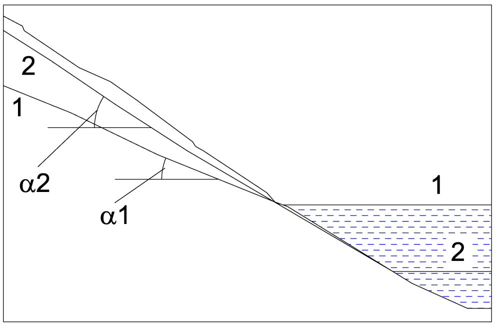

Figure 6: Sketch, hydraulic gradient

Seasonal changing influences
To get seasonal changing displacement velocity we need seasonal changing boundary conditions. The most obvious changing boundary condition is the ground water flow. During winter there is low ground water flow which raises in spring with snow melt and rain. Especially in combination with the seasonal changing storage water level, we have a higher hydraulic gradient (α_2) in spring (low storage water level and high ground water flow, case 2 in Figure 6) and a lower hydraulic gradient (α_1) in autumn (high storage water level and lower ground water flow, case 1 in Figure 6). The hydraulic gradient is the slope of the water table. The seepage forces depend on the hydraulic gradient as follows:

$$F_s = i\gamma_w V$$

with the seepage force F_s, the hydraulic gradient i, the bulk density of the fluid γ_w and the seeped volume V.

With a higher hydraulic gradient, the seepage forces become higher and with this the stress level raises. The stress tensor comprises the self weight of the material and the stresses out of seepage. This means we get a seasonal changing stress tensor.

Results
As has been shown in (Schneider-Muntau et al., 2006) a linear relation between stress and strain rate in not sufficient to describe the behaviour of the slope ($v_2/v_1 = 1.65$). Therefor this nonlinear creep law has been fitted to the laboratory experiments. An exponent n=2.2 leads to displacement velocities which are 4.6 times higher during spring than during autumn. This correlates much better with the ratio of measured displacement rates in situ ($v_2/v_1 = 3.0 - 7.2$).

Conclusion

The potential function can be fitted to the laboratory experiments. Still a great scatter can be seen on the results. There are still creep tests going on which have to be evaluated once they are finished. With more results the spread of the results might become closer. As the measured displacement rates show a nonlinear dependence, the nonlinear correlation of the stresses and the strain rates in the finite element calculation represents the behaviour better and leads to results closer to reality.

Acknowledgement

The authors wish to thank the ILF – Consulting Engineers and TIWAG – Tyrolean Hydro – electric Power Co. for their kind support of this work and the TIWAG also for providing the good data set for the analysis.

References

H. Breth. The dynamics of a landslide produced by filling a reservoir. *Commission Intrenationales der Grands Barrages*, 9:37–45, 1967.

E. Brückl, C. Zangerl, and E. Tentschert. Geometry and deformation mechanisms of a deep seated gravitational creep in crystalline rocks. *EUROCK 2004, Salzburg, Austria*, 2004.

E. Hoek. Putting numbers to geology - an engineer's viewpoint. *The second Glossop Lecture - Q. J. Engrg. Geol.*, 32:1–21, 1999.

L. Müller. *Der Felsbau*, volume 1. Maisch und Queck, Gerlingen, 1963. Theoretischer Teil.

L. Müller. *Der Felsbau*, volume 2. Ferdinand Enke Verlag, 1992. Felsbau über Tage, 2. Teil, Gründung, Wasserkraftanlagen (1. Abschnitt).

D. Renk. Geotechnische Untersuchungen von Gleitzonenmaterialien großer Hangbewegungen. Master's thesis, Universität Karlsruhe (TH), Universität Innsbruck, 2006.

B. Schneider-Muntau, C. Zangerl, and W. Fellin. Hydromechanical coupled finite element modelling of a slowly creeping landslide. *3rd Colloquium Rock Mechanics, Theory and Practice, Vienna*, 2006.

S. Semprich and B. Plischke. *Felsmechanik*. Springerverlag, 1984. Grundlagen für wirtschaftliches Bauen im Fels.

A. Spickermann, T. Schanz, and M. Datcheva. Numerical study of a potential landslide in the swiss alps. *5th EUROMECH Solid Mechanics Conference*, 2003.

E. Tentschert. *Das Langzeitverhalten der Sackungshänge im Speicher Gepatsch (Tirol, Österreich)*, volume 16. Felsbau, 1998. 194-200.

TU Darmstadt. Laboratory experiments. Technical report, Institute and Laboratory of Geotechnics, Faculty of Civil Engginеering and Geodesy, 1964.